**Electronic Supplementary Information**

# Layer-by-Layer Integration of Conducting Polymers and Metal Organic Frameworks onto Electrode Surfaces: Enhancement of the Oxygen Reduction Reaction through Electrocatalytic Nanoarchitectonics

Ana Paula Mártire, Gustavo M. Segovia, Omar Azzaroni,* Matías Rafti,* and Waldemar Marmisollé[1]

Instituto de Investigaciones Fisicoquímicas Teóricas y Aplicadas (INIFTA), Departamento de Química, Facultad

de Ciencias Exactas, Universidad Nacional de La Plata (UNLP), CONICET, (1900) La Plata, Argentina.

[1] E-mail: azzaroni@inifta.unlp.edu.ar (O.A.)
  E-mail: mrafti@quimica.unlp.edu.ar (M.R.)
  E-mail: wmarmi@inifta.unlp.edu.ar (W.A.M.)

## 1. X-Ray Photoelectron Spectroscopy

XPS was performed using a SPECS SAGE HR 100 system spectrometer. A Mg Kα (1253.6 eV) X-ray source was employed operating at 12.5kV and 10mA. Survey spectra were obtained with pass energy of 30 eV whereas 15 eV was employed for detailed spectra of C1s, N1s, S2p and Zn2p regions. Quantitative analysis of spectra was performed with the software Casa XPS 2.3. 16 PR 1.6. Surface-charging effects were corrected by setting the binding energy (BE) of the main component of the core level C1s at 284.5 eV.[1] The full width at half maximum (fwhm), was kept fixed for different components of a given element.

Samples analyzed by XPS were Pani-PSS complex and PAH-ZIF-8 powders and Pani-PSS/PAH-ZIF-8 1 bilayer assembly. Results are presented in **Fig. S1**.
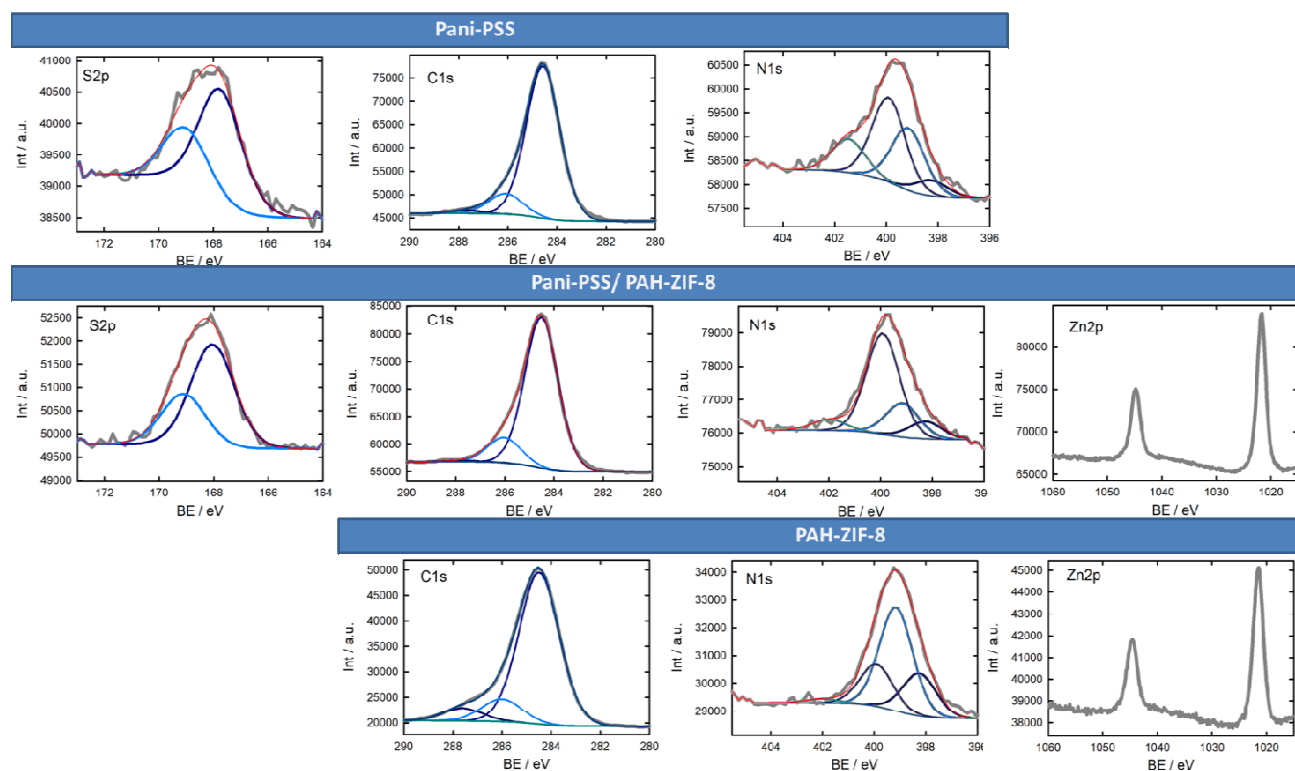


**Figure S1.** S2p , C1s, N1s and Zn2p core regions of XPS spectra of solid Pani-PSS complex, Pani-PSS/PAH-ZIF-8 (1 bilayer assembly) and PAH-ZIF-8 powder.

The XPS spectra of C1s core regions can be deconvoluted employing 3 components (**Table S1**). The main component is assigned to aliphatic and aromatic CH, CC and simple uncharged CN bonds and it was set at 284.5 eV for BE calibration.[1] The next component at 286 eV can be assigned to charged nitrogen (CN+/C=N+),[2] whereas the minor component at BE>287 eV can be assigned to C bound to O, due to oxidized units and contamination.[2,3]

The sulphur signal (S2p) in Pani-PSS-containing samples appears at about 169 eV and can be fitted to a set of two bands assigned to $S2p_{3/2}$ and $S2p_{1/2}$ with an integrated area ratio of 0.5 which takes into account the degeneration of these levels.[4]

N1s core spectra were deconvoluted into 4 peaks (fwhm 1.5 eV) (**Table S2**). The backbone N atoms can be considered to contribute with 4 bands corresponding to the uncharged N species in Pani and imidazole (neutral imine[1–3,5] and neutral amine[2,3], pyridinic and pyrrolic species[6]) and positive N species from oxidized secondary amines in Pani-PSS (delocalized polaron-type structure)[3,5,7] and protonated imine (localized bipolaron-type structure)[2,3] or N coordinated to cationic species($N(\delta^+)$).[6]

Finally, the peaks assigned to Zn2p core level appear at 1022 ($2p_{3/2}$) and 1044 eV ($2p_{1/2}$), which is typical of ZIF-8 materials. [8]

**Table S1.** C1s core components used for fitting (fwhm=1.6 eV) and atomic composition.

| | C1s | CH/CC/C-N | C=N/C=N+ | CO/C=O |
|---|---|---|---|---|
| **Pani-PSS** | BE / eV | 284.5 | 286.1 | 287.7 |
| | % | 87 | 12 | 2 |
| **Pani-PSS/PAH-ZIF-8** | BE / eV | 284.5 | 286.0 | 287.6 |
| | % | 85 | 14 | 1 |
| **PAH-ZIF-8** | BE / eV | 284.5 | 286.0 | 287.6 |
| | % | 81 | 12 | 7 |

**Table S2.** N1s core components used for fitting (fwhm=1.5 eV) and atomic composition.

| | N1s | -N= | NH/NH2 | $-N^{·+}-$ /$NH_3+$/$N(\delta^+)$ | -NH+= |
|---|---|---|---|---|---|
| **Pani-PSS** | BE / eV | 398.2 | 399.1 | 399.9 | 401.5 |
| | % | 8 | 32 | 43 | 17 |
| **Pani-PSS/PAH-ZIF-8** | BE / eV | 398.3 | 399.2 | 399.9 | 402.0 |
| | % | 10 | 21 | 62 | 7 |
| **PAH-ZIF-8** | BE / eV | 398.3 | 399.1 | 399.9 | |
| | % | 22 | 54 | 22 | |

## 2. QCM experiments

In situ assembly of the nanoarchitecture proposed was carried by Quartz Crystal Microbalance (QCM). QCM measurements were performed with a QCM200 Quartz Cristal Microbalance equipped with Gold QCM25 5 MHz oscillators (Sensitivity factor: 56.6 Hz cm$^2$ µg$^{-1}$) (Stanford Research Systems). Determinations were performed with quiescent solutions in a Teflon cell.

**Fig. S2** shows the evolution of relative frequency as the number of cycles preformed increments. **Table S3** shows the values of relative frequency in Hz and the corresponding mass per unit area from which the mean ratio of mass deposition of the assembly was determined to be $r$= m(Pani-PSS)/m(ZIF-8-PAH)=0.81
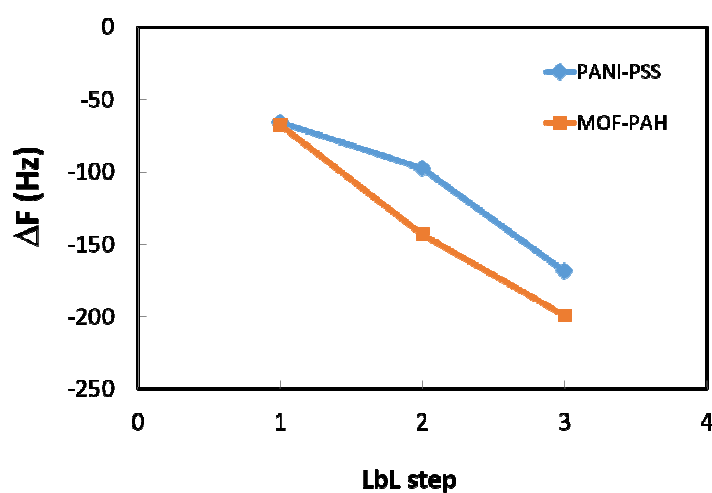


**Figure S2.** Frequency change for the LbL assembly of conducting polymer and MOF composite. Values of each deposition step for negative (Pani-PSS) and positive (PAH-ZIF-8) building blocks corresponding to 3 deposition cycles are presented.

**Table S3.** Frequency change and mass per unit area increment for the LbL presented in **Fig. S2**.

| # LbL cycle | Pani-PSS step | | PAH-ZIF-8 step | | Total | |
|---|---|---|---|---|---|---|
| | ΔFreq. (Hz) | mass (ug cm$^{-2}$) | ΔFreq. (Hz) | mass (ug cm$^{-2}$) | ΔFreq. (Hz) | mass (ug cm$^{-2}$) |
| 1 | -65.5 | 1.157 | -67.7 | 1.196 | -133.2 | 2.353 |
| 2 | -97.6 | 1.724 | -143 | 2.526 | -240.6 | 4.251 |
| 3 | -168.7 | 2.981 | -198.9 | 3.514 | -367.6 | 6.495 |

## 3. Electrochemistry of nanocomposite electrodes formed by bulk casting.

In order to study the influence of the nanoarchitectonic integration on the effect of enhancement of the ORR, the LbL approach was compared with the direct aggregation of both components. For this purpose, aggregates were prepared by mixing dilute solutions of Pani-PSS and PAH-ZIF-8 dispersions, keeping the mass proportion determined by QCM. The aggregates were then deposited on Au/PEI electrodes by drop-casting. **Fig. S3 (a)** shows the voltammetric response of the aggregates-modified electrode and a 1- bilayer Pani-PSS/PAH-ZIF-8-modified electrode. The ORR response of these electrodes is presented in **Fig. S3 (b)**.

The voltammetric integrated charge corresponding to the cathodic peak of the Pani-PSS component is *ca.* 6 times higher in the case of the electrode modified with the aggregates **(Fig. S3 (a))**; however, the ORR current is practically the same (and even higher) for the LbL assembly. The ORR integrated charge due to the ORR normalized to the amount of electroactive material is then *ca.* 6 times higher in the case of the LbL integration approach. This result confirms that the LbL approach allows the effective integration of low amounts of the electroactive components.
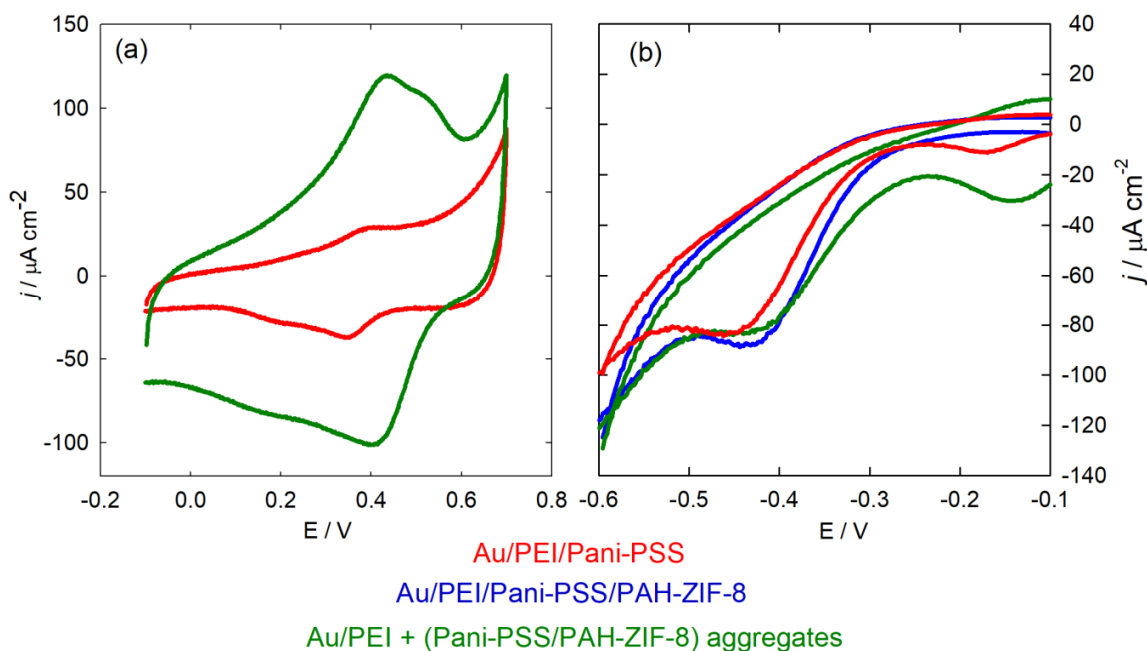
**Figure S3. (a)** Comparison of the voltammetric responses of a single Pani-PSS layer on Au/PEI electrode modified by dip-coating (red), and Au/PEI electrode modified with Pani-PSS/PAH-ZIF-8 aggregates deposited by drop-casting (green). **(b)** Cyclic voltammograms at 10 mV s$^{-1}$ in the ORR region in air-saturated 0.1 M KCl solution of Au electrodes after functionalization with Pani-PSS (red), Pani-PSS/PAH-ZIF-8 formed by LbL assembly (blue), and aggregates deposited by drop-casting (green).

### References

1   J. Yue and A. Epstein, *Macromolecules*, 1991, **24**, 4441–4445.

2   S. Golczak,  a Kanciurzewska, M. Fahlman, K. Langer and J. Langer, *Solid State Ionics*, 2008, **179**, 2234–2239.

3   S. Kumar, F. Gaillard, G. Bouyssoux and A. Sartre, *Synth. Met.*, 1990, **36**, 111–127.

4   W. A. Marmisollé, E. Maza, S. Moya and O. Azzaroni, *Electrochim. Acta*, 2016, **210**, 435–444.

5   C. Hennig, K. H. Hallmeier and R. Szargan, *Synth. Met.*, 1998, **92**, 161–166.

6   Y. Li, X. Cai, S. Chen, H. Zhang, K. H. L. Zhang, J. Hong, B. Chen, D. H. Kuo and W. Wang, *ChemSusChem*, 2018, **11**, 1040–1047.

7   E. Kang, K. Neoh and K. Tan, *Polymer*, 1994, **35**, 3193–3199.

8   R. L. Papporello, E. E. Miró and J. M. Zamaro, *Microporous Mesoporous Mater.*, 2015, **211**, 64–72.